MIT Open Access Articles

Design of BET Inhibitor Bottlebrush Prodrugs with Superior Efficacy and Devoid of Systemic Toxicities

The MIT Faculty has made this article openly available. ***Please share*** how this access benefits you. Your story matters.

Citation	2021. "Design of BET Inhibitor Bottlebrush Prodrugs with Superior Efficacy and Devoid of Systemic Toxicities." Journal of the American Chemical Society, 143 (12).
As Published	10.1021/JACS.1C00312
Publisher	American Chemical Society (ACS)
Version	Author's final manuscript
Citable link	https://hdl.handle.net/1721.1/141089
Terms of Use	Creative Commons Attribution-Noncommercial-Share Alike
Detailed Terms	http://creativecommons.org/licenses/by-nc-sa/4.0/

Massachusetts Institute of Technology

DSpace@MIT

Author Manuscript

Author Manuscript

Author Manuscript

Author Manuscript

HHS Public Access

Author manuscript

J Am Chem Soc. Author manuscript; available in PMC 2021 July 28.

Published in final edited form as:

J Am Chem Soc. 2021 March 31; 143(12): 4714–4724. doi:10.1021/jacs.1c00312.

Design of BET Inhibitor Bottlebrush Prodrugs with Superior Efficacy and Devoid of Systemic Toxicities

Farrukh Vohidov[#1], **Jannik N. Andersen**[#2], **Kyriakos D. Economides**[2], **Michail V. Shipitsin**[2], **Olga Burenkova**[2], **James C. Ackley**[2], **Bhavatarini Vangamudi**[2], **Hung V.-T. Nguyen**[1], **Nolan M. Gallagher**[1], **Peyton Shieh**[1], **Matthew R. Golder**[1], **Jenny Liu**[1,2], **William K. Dahlberg**[2], **Deborah J. C. Ehrlich**[1], **Julie Kim**[1], **Samantha L. Kristufek**[1], **Sung Jin Huh**[2], **Allison M. Neenan**[2], **Joelle Baddour**[2], **Sattanathan Paramasivan**[2], **Elisa de Stanchina**[3], **KC Gaurab**[2], **David J. Turnquist**[2], **Jennifer K. Saucier-Sawyer**[2], **Paul W. Kopesky**[2], **Samantha W. Brady**[2], **Michael J. Jessel**[2], **Lawrence A. Reiter**[2], **Donald E. Chickering**[2], **Jeremiah A. Johnson**[1,*], **Peter Blume-Jensen**[2,4,*]

[1]Department of Chemistry, Massachusetts Institute of Technology, 77 Massachusetts Avenue, Cambridge, Massachusetts 02139, United States

[2]XTuit Pharmaceuticals, 35 Gatehouse Drive, Waltham, Massachusetts 02451, United States

[3]Memorial Sloan Kettering Cancer Center, 417 E 68th St, New York, NY 10065, United States

[4]Current Address: Acrivon Therapeutics, Lab Central, 700 N. Main Street, Cambridge, MA 02139, United States

[#] These authors contributed equally to this work.

Abstract

Prodrugs engineered for preferential activation in diseased versus normal tissues offer immense potential to improve the therapeutic indexes (TIs) of preclinical and clinical-stage active pharmaceutical ingredients that either cannot be developed otherwise or whose efficacy or tolerability it is highly desirable to improve. Such approaches, however, often suffer from trial-and-error design, precluding predictive synthesis and optimization. Here, using bromodomain and extra-terminal (BET) protein inhibitors (BETi)—a class of epigenetic regulators with proven anti-cancer potential but clinical development hindered in large part by narrow TIs—we introduce a macromolecular prodrug platform that overcomes these challenges. Through tuning of traceless linkers appended to a “bottlebrush prodrug” scaffold, we demonstrate correlation of *in vitro* prodrug activation kinetics with *in vivo* tumor pharmacokinetics, enabling the predictive design of novel BETi prodrugs with enhanced anti-tumor efficacies and devoid of dose-limiting toxicities in a syngeneic triple-negative breast cancer murine model. This work may have immediate clinical implications, introducing a platform for the predictive prodrug design and potentially overcoming hurdles in drug development.

[*]Corresponding Authors: J.A. Johnson: jaj2109@mit.edu; P. Blume-Jensen: pblumejensen@acrivon.com.

Competing interests: F.V. and J.A.J. are named inventors on patent applications filed by the Massachusetts Institute of Technology on the linker compositions and bottlebrush polymer platform described in this work.

Supporting Information: Supporting figures, methods, materials, procedures, spectra, and characterization data.

Author Manuscript Author Manuscript Author Manuscript Author Manuscript

Graphical Abstract

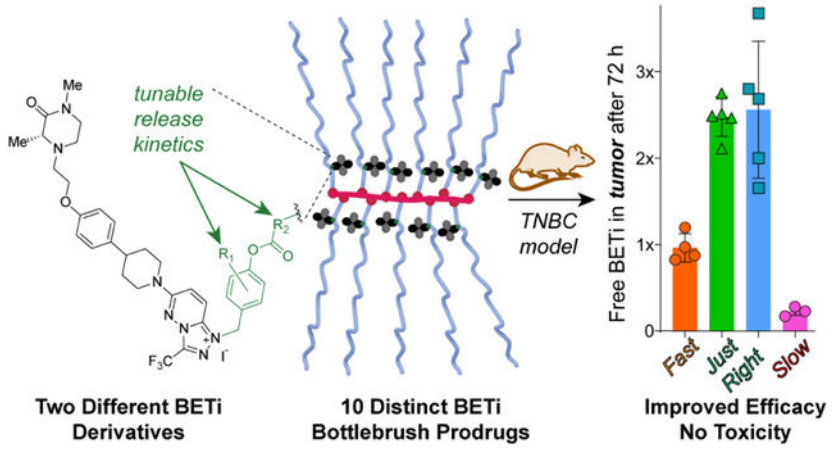

Introduction.

Medicinal chemistry optimization to deliver a drug candidate for clinical testing and ultimate regulatory approval is an essential part of drug discovery.[1–3] This process, which often fails, is typically costly and time consuming and often follows trial-and-error optimization, leading to a trade-off between orthogonally-trending properties such as target potency, solubility, metabolic stability, and toxicity.[4–5] For example, bromodomain and extra-terminal motif protein inhibitors (BETis) have been the subject of intense medicinal chemistry efforts, displaying broad preclinical efficacies[6–7] *in vivo*, as well as clinical activities in various cancers, including notably myelofibrosis.[8–9] BETi treatment has been shown to induce drug-dependent decreases in the expression of oncogenes such as c-MYC[10–11] and cyclin-dependent kinases.[12–14] To date, at least 23 structurally distinct BETi have been evaluated in >46 human clinical trials, demonstrating the clinical efficacy of this class of drugs. Nevertheless, a review of www.clinicaltrials.gov from January 2017 to May 2020 indicates that most of these programs report protracted phase I/II development times and reduced patient enrollment targets due to severe dose-limiting toxicities (DLTs) (Supplementary Table 1). For example, the prototypical benzodiazepine BETi OTX-015 (MK-8628, Merck)[15–17] causes thrombocytopenia (96%), anemia (91%), and neutropenia (51%), with additional gastro-intestinal adverse events (diarrhea, vomiting and mucositis).[18] Similar treatment-related adverse effects have been reported for the structurally distinct bivalent BETi, AZD5153.[19–20] Given the promising clinical activity of this drug class, we envisioned that a prodrug approach to improve the therapeutic indexes (TIs) of existing clinical and preclinical BETi could provide an immediately actionable strategy to enable their successful clinical development.

The development of covalent drug-delivery systems, or prodrugs, often also involves trial-and-error design due to unpredictable active pharmaceutical ingredient (API)–carrier interactions, limited synthetic scalability and modularity, and unpredictable or poorly controlled drug release profiles.[21–22] Here, we introduce a modular, scalable, and well-defined bottlebrush prodrug (BPD) platform that overcome these challenges as demonstrated

Author Manuscript Author Manuscript Author Manuscript Author Manuscript

in the context of BETis. Through the synthesis of BETi-BPDs carrying either OTX-015 or a bivalent BETi "T-API" conjugated through molecularly optimized, traceless linkers, we exemplify an accelerated method to improve the TI of BETi as demonstrated using orthotopically implanted, immune-competent tumor-bearing mice. This work establishes BPDs as a promising solution for small molecule API delivery to overcome DLTs and improve the safety profile for compounds with proven clinical activity (as demonstrated for OTX-015) and for the accelerated development of novel lead candidates (as demonstrated using T-API).

Results.

Downregulation of the c-Myc oncogene and subsequent cell cycle arrest has been proposed as a major mechanism for BETi-mediated tumor growth inhibition;[10, 23–24] however, downregulation of c-Myc in normal tissues, including gut and hematopoietic precursors in bone marrow, results in clinically observed on-target DLTs.[25–26] We hypothesized that improved delivery of BETi-BPDs to tumors combined with the design of linkers with favorable API release in the tumor microenvironment compared to blood and other healthy tissues would be key parameters to improve the TI. To test this hypothesis, OTX-015 offered an attractive starting point for BETi-BPD development, given the inferior TI of this compound that has hindered its successful clinical development.

Optimization of API release rates through traceless linker editing.

OTX-015 contains a phenolic substituent suitable for direct conjugation to polyethylene glycol (PEG)-*branch*-alkyne macromonomers (MMs) that constitute the basic building blocks of the BPD platform (Fig. 1a). Four different azido acids (shown in blue, Fig. 1a) were used to prepare four OTX-015-conjugated macromonomers (MMs) with *in vitro* half-lives of OTX-015 release ($t_{1/2,MM}$) of 5 h (**B1 MM**) to 6 d (**B4 MM**) in phosphate-buffered saline at 37 °C (Fig. 1b,c). BETi-BPDs **B1**–**B4** were prepared through ring-opening metathesis polymerization (ROMP)[27–30] of each MM at a target degree of polymerization (DP) of 10. 1 mol % of Cy7.5 fluorophore-labeled MM[31] was included in all ROMP reactions to enable downstream *in vivo* tissue imaging studies to supplement our quantitative pharmacokinetics (PK) analyses for accurate biodistribution (BD) assessment. Near complete conversions of each MM to BETi-BPD were observed (Fig. S1). The intensity-averaged hydrodynamic diameters (D_h) of each BPD were ~10 nm as determined by dynamic light scattering (DLS) (Fig. S2a,b). This size range is comparable to therapeutic antibodies and ADCs, offering potentially optimal BD, PK, and disease tissue penetration. Moreover, while release from BPDs was much slower than for MMs, overall trends were conserved as measured for **B1** and **B4** (Fig. S2c). In support of the scalability of our synthetic approach, 4 g of BETi-BPDs were prepared for subsequent biological studies (Fig. S3). As expected for BPDs where the APIs are shielded by hydrophilic PEG, the half-maximal inhibitory concentrations (IC_{50}) for **B1**–**B4** were approximately one order-of-magnitude higher compared to the parent API based on *in vitro* cell viability assays using either bone marrow $CD34^+$ progenitor cells (erythroid, megakaryocyte, and myeloid), human aortic endothelial cells, lymphoma (SU-DHL-2) or breast cancer (4T1) cells (Fig. S4,5)

Author Manuscript Author Manuscript Author Manuscript Author Manuscript

To correlate the pharmacological properties of BETi-BPDs *in vivo* with the MM release kinetics measured *in vitro*, we dosed BALB/c mice orthotopically implanted with syngeneic 4T1 tumors with **B2**–**B4** and collected blood samples at multiple time points for PK analysis by mass spectrometry (MS). As shown in Fig. 1d, **B4** was relatively stable in blood with a minimal peak free drug serum concentration detected 30 min after administration, which is significantly lower than the peak concentrations at 2 and 3 h post dosing of maximally tolerated doses (MTD) of OTX-015. By contrast, **B2** and **B3** displayed 2–3 times higher concentrations of free OTX-015 in serum. **B1** was not evaluated *in vivo* due to its rapid API release in buffer (Fig. 1c, Fig. S2b). In parallel to the blood analyses, the tumor tissue concentrations of free OTX-015 were quantified 72 h post dose (Fig. 1e). The tumor API levels released from **B4** at 72 h were comparable with the tumor drug concentrations at 2 to 3 h after oral administration (Fig. 1e). Thus, **B4** exhibits long-term release of OTX-015 in tumor tissue for at least up to 72 h while maintaining a low serum concentration, suggesting that it may display an improved TI.

To further confirm that the different tumor concentrations of released API from **B2**, **B3**, and **B4** are primarily due to their linker design rather than differences in their overall biodistribution, *ex vivo* near-infrared fluorescence imaging of tissue samples was conducted to determine the amount of Cy7.5 fluorophore-labeled prodrug present in each tissue. All three BETi-BPDs (**B2**, **B3**, and **B4**) showed similar accumulation in tumor tissue based on whole tumor analysis (Fig. S6). Importantly, fluorescence imaging of intact tumors and organs and of homogenized tissues showed preferential distribution of BETi-BPDs to orthotopic tumors and only negligible levels of Cy7.5 in bone marrow and the gut—organs associated with the DLTs of OTX-015 (Fig. 2a,b). These results, combined with the *in vitro* release kinetics for **B4**, demonstrate that it is possible to chemically fine-tune both the BD of, and API release from, BETi-BPDs to minimize systemic exposure while maintaining, or even improving, tumor exposure of the active drug over long time periods.

Superior anti-tumor efficacy of B4 *in vivo*.

We next evaluated the anti-tumor efficacy of **B4** in the aggressive 4T1 syngeneic, orthotopic model, which features a realistic immune response and tumor microenvironment, recapitulating many features of late stage triple-negative breast cancer (TNBC) in humans. The functioning adaptive immune system of these mice provides an opportunity to study potential treatment-related immunosuppressive adverse effects that are lost with more common xenograft models using immunocompromised mice. A dose escalation study using **B4** was conducted in randomized, tumor-bearing BALB/c mice dosed with equivalents of OTX-015 at 15, 30, or 60 mg/kg twice per week for two weeks for a total of 4 doses, or at 60 mg/kg three times per week for two weeks for a total of 6 doses (Fig. 2c). Two separate control cohorts were dosed for 14 days with free OTX-015 twice a day by oral gavage (bid; po) at 100 or 200 mg/kg, respectively, mimicking the clinical route of administration.

A dose-proportional anti-tumor efficacy was observed for mice administered **B4**, with highly effective tumor growth inhibition at higher doses (Fig. 2d). At the 60 mg/kg OTX-015 equivalent dose of **B4,** both the 4× and 6× regimens showed superior anti-tumor efficacy compared to the highest daily tolerated dose of OTX-015 (100 mg/kg bid). Notably, the total

Author Manuscript Author Manuscript Author Manuscript Author Manuscript

amount of OTX-015 in the group that received the highest dose of **B4** was ~360 mg/kg, which is >*7-fold less than* that of the group given OTX-015 at 100 mg/kg bid (2800 mg/kg after two weeks) (Fig. 2d). We attribute the enhanced efficacy **B4** with less dosage-equivalent of API to a linker-optimized depot effect,[32] wherein **B4** accumulates in tumor tissue and releases therapeutically relevant concentrations of OTX-015 over longer time periods than what is achievable with OTX-015, even when dosed twice daily. To support this concept, MS analyses of homogenized tumor samples (Fig. 2e) revealed high levels (~100 μg/g) of **B4** (BETi-BPD) and ~3 orders-of-magnitude lower levels of released OTX-015 (~1500 ng/g). Moreover, the amount of **B4** and released API in tumor samples scaled proportionally with dosage (Fig. 2e). Notably, the concentration of free OTX-015 72 h after **B4** injection is still almost 50% of the peak concentration in tumors achieved from non-tolerated orally dosed OTX-015 obtained 2 h post dosing and much greater than the concentration of oral OTX-015 at MTD, which is cleared from the tumor tissue and cannot be detected after 24 h (Fig. 2e). As a direct consequence of the optimal BD and API release from **B4**, no weight loss was observed in any of the groups receiving **B4**, while the group receiving free OTX-015 at 200 mg/kg had to be sacrificed early due to severe weight loss (>20%); the group receiving the highest tolerated dose of API at 100 mg/kg experienced diarrhea and modest (~5%) weight loss after 2 weeks of chronic dosing (Fig. 2f).

BETi-BPDs releasing OTX-015 exhibit enhanced anti-tumor efficacy without dose-limiting bone marrow and intestinal toxicities.

Detailed analyses of cell populations in terminal blood and bone marrow collected from the above efficacy study demonstrated that animals dosed with **B4** were spared from the systemic DLTs normally associated with clinical BET inhibition (Fig. 3a, Fig. S7). Specifically, platelet, reticulocyte, neutrophil, and lymphocyte levels were not affected in mice treated with **B4** compared to the group treated with OTX-015. Moreover, gut and tumor tissue samples were collected for immunohistochemical analyses (Fig. 3b). **B4** induced minimal intestinal toxicity compared to OTX-015, as evidenced by preserved colonic villus epithelial cell surface morphology and *in situ* expression of c-Myc in the base of crypts. Consistent with the anti-tumor efficacy of **B4**, a robust modulation of known pharmacodynamic (PD) markers was observed in tumor tissue, with downregulation of c-Myc and CD180 and upregulation of HEXIM1[33] (Fig. 3b,c, Fig. S8). In conclusion, **B4** represents a promising OTX-015 prodrug with an expanded TI and improved efficacy following infrequent dosing. Its development was enabled by the modularity of the BPD platform, which led us to consider applying the same approach to a structurally distinct BETi with poor drug-like properties.

The BPD platform applied to preclinical (triazolopyridizine-based) bivalent BETi.

AstraZeneca reported a triazolopyridazine[20] class of potent BETis that are structurally distinct from OTX-015, comprising bivalent ligands that engage both of the bromodomains[34] of the BET family of proteins and displaying higher potencies in cell-based assays compared to many of the small-molecule inhibitors derived from the benzodiazepine scaffold. AZD5153, a bivalent BETi with optimized PK properties, is currently undergoing clinical trials.[19] For our study, we selected an AZD5153 derivative “T-API” (Fig. 4a), which

Author Manuscript Author Manuscript Author Manuscript Author Manuscript

features a trifluoromethyl substituent in place of a methoxy group. While T-API has similar *in vitro* potency compared to AZD5153 (Fig. S5, S9) (IC_{50} < 100 nM) against a multiple myeloma (MM1.S) cell line, it suffers from poor physicochemical properties such as low aqueous solubility (<0.05 mg/mL), high lipophilicity (log $D_{7.4}$ > 4.2), and inadequate hepatocyte stability (70 heps Cl_{int} mL/min/10^6 cells),[20] all of which are largely prohibitive for activity *in vivo* (Fig. S10). Indeed, we found that blood levels of T-API in BALB/c mice (n = 3) were significantly lower compared to AZD5153 (1000 ng/mL vs. 5000 ng/mL) 2 h after 10 mg/kg i.v. administration, and the exposure dropped to negligible levels within 4 h (Fig. S11a), most likely due to rapid metabolism in the liver[20] (Fig. S12). Having already demonstrated that our BPD platform provides for both favorable delivery of BETi-BPDs and subsequent API release in tumor tissues, we next evaluated whether we could apply the same approach to improve the efficacy of T-API, which suffers from low metabolic stability and rapid clearance.

Unlike OTX-015, T-API (Fig. 4a; black structure) does not offer an obvious synthetic handle for conjugation. To address this challenge, and inspired by recent amide-based linkers for N-containing drugs,[35–36] we developed a new class of phenyl ester linkers based on the quaternization of nitrogen-containing heterocycles using benzyl iodides (Fig. 4a; blue structure). For these linkers, prodrug activation is dependent on the rate-determining cleavage of a *para*-aryl ester, which can be tuned through predictable modifications to the ester, followed by a 1,6-elimination cascade,[37–40] releasing the drug via *N*-debenzylation (Fig. 4a). The desired T-API-based triazolopyridazinium salts were synthesized in 50–70% isolated yields following optimized benzylation procedures (see Supplementary Materials for details; Fig. S13, S14). Their structures were unambiguously determined by 2D NMR spectroscopy (Materials and Methods). Regardless of the linker used, quaternization was observed to occur on the same nitrogen atom of the 1,2,4-triazole of T-API. The T-API conjugates were converted to MMs and later to their corresponding DP ~ 10 BETi-BPDs via ROMP (Fig. S1, Fig. S2a).

Using this novel conjugation strategy and linkers with varied steric and electronic properties, we initially prepared four different T-API-conjugated MMs with $t_{1/2,MM}$ ranging from hours (**T1 MM**) to days (**T2 MM**) to months (**T3 MM** and **T4 MM**) (Fig. 4b) as confirmed by *in vitro* drug release assays (saline buffer, 37 °C) (Fig. 4c). For each linker, free T-API was observed to be the sole species released upon hydrolysis (Fig. S15), suggesting 1,6-elimination occurs rapidly under these conditions. Following i.v. administration (60 mg/kg × 4 of T-API equivalent) to mice bearing 4T1 tumors, **T3** and **T4** showed negligible to low levels of free T-API in tumor tissues (Fig. 4d), perhaps as expected due to the slow hydrolysis of their linkers. By contrast, **T2** released much higher concentrations of T-API in tumor tissue and provided a tumor-to-blood ratio of 2:1 (Fig. 4e), making it the preferred linker of this series (note: **T1** was not studied *in vivo* due to its very rapid release kinetics). For subsequent *in vivo* studies, the clinical candidate AZD5153 was selected as the benchmark for the T-API prodrug since the poor drug-like properties of free T-API are not compatible with *in vivo* efficacy studies (Fig. S11, S12). Consistent with the clinical dosing schedule (daily or twice daily) for AZD5153,[19] this API was not detectable 24 h after administration (Fig. S11b). By contrast, the PK profile in blood following a single dose of

Author Manuscript Author Manuscript Author Manuscript Author Manuscript

T2 (15 mg/kg T-API equivalent, i.v.) demonstrated that the BETi-BPD released only very low levels of T-API in blood with a peak concentration significantly lower than that of the rapidly cleared AZD5153 (Fig. S11b).

Similar to the OTX-015 derived **B4**, **T2** displayed favorable tumor accumulation based on Cy7.5 imaging (Fig. 5a,b). Additionally, **T2** (dosed i.v. with equivalent of T-API at 60 mg/kg × 6, 360 mg/kg cumulative dose) showed better anti-tumor efficacy compared with a maximum tolerated daily dose (qd) of AZD5153 (10 mg/kg, p.o. 130 mg/kg cumulative dose; Fig. 5c and 5d), which is notable given that the latter compound underwent extensive medicinal chemistry optimization compared to T-API. To further validate the critical nature of the **T2** linker, prodrugs **T3** and **T4** (60 mg/kg × 4) were also tested in the same tumor model. These constructs displayed no antitumor efficacy (Fig. S16), consistent with MS analysis of extracted tumors showing minimal release of free T-API despite similar levels of **T3** and **T4** prodrugs in tumor compared to **T2** (Fig. S17). **T2** generated therapeutically relevant and superior concentrations of T-API that remained at high concentrations (~10× more) in tumor tissue 72 h following administration. These results show that the tumor accumulation of our BPDs is not dependent on the linker structure, allowing for fine-tuning of release kinetics independently of BD. As was observed for OTX-015, negligible levels of AZD5153 were detectable in tumor tissue after 24 h (Fig. 5e). Importantly, mice administered the high dose of **T2** (60 mg/kg × 6) displayed no weight loss and normal, healthy livers, highlighting the safety of our prodrug (Fig. 5f, S18). While AZD5153 also achieved objective tumor responses when dosed at 5–20 mg/kg (po, qd; 65–360 mg/kg cumulative doses), these animals experienced significant body weight loss and the group receiving 20 mg/kg had to be taken down before the end of the study. In contrast to the MTD dose group (10 mg/kg po qd of AZD5153), which led to significant reductions in white blood cell, platelet, and reticulocyte counts, **T2** displayed no discernible blood toxicity (Fig. 6a). Moreover, detailed analysis of gut and tumor samples demonstrated that **T2** lowers c-Myc levels in tumors but not in the gut, while AZD5153 displayed PD biomarker modulation in both tumor and gut epithelial tissue (Fig. 6b,c). Overall, these results for **T2** mirror those of **B4** yet with a structurally different BETi, suggesting that our platform, which embeds APIs near the backbone of a bivalent bottlebrush polymer, possesses “drug-agnostic” physical properties that can be leveraged to accelerate the predictable development of APIs with poor drug-like properties without protracted medicinal chemistry optimization.

To take our system a step further, we sought to investigate whether or not further fine-tuning of linker structures could provide even greater tumor:blood ratios for T-API. Closer analysis of the tumor PK data for **B4** and **T2** (Fig. 2e and 5e, respectively) revealed much less **T2** and free T-API 72 h after administration compared to **B4** and free OTX-015, suggesting that the rate of linker cleavage for **T2** may be unnecessarily high despite its excellent *in vivo* efficacy and safety. Based on this insight, we designed and synthesized two new variants of **T2** with electron donating *ortho*-methoxy (**T2-OMe**) and *ortho*-methyl (**T2-Me**) substituents (Fig. 4b) that are expected to slow the rate of ester hydrolysis.[37] As predicted, *in vitro* release assays revealed a doubling of the $t_{1/2,MM}$ values to ~5 and ~6 days for **T2-OMe MM** and **T2-Me MM**, respectively (Fig. 4c), and the BPD **T2-OMe** had a similar release profile compared to the optimal OTX-015 BPD **B2** (Fig. S2c), confirming that such design can be

Author Manuscript Author Manuscript Author Manuscript Author Manuscript

used to fine tune T-API release in this system. Moreover, tumor and blood PK studies showed further improved T-API release (Fig. 4d) and higher tumor:blood ratios (up to ~5 compared to ~2 for **T2**, Fig. 4e) for these constructs compared to **T2**. In agreement with these improved tumor PK results, *lower* doses of **T2-OMe** (60 mg/kg × 4) and **T2-Me** (60 mg/kg × 4) compared to **T2** (60 mg/kg × 6) led to improved or similar tumor growth inhibition (Fig. 7a,b), respectively, and no gross toxicity (Fig. 7c) compared to a high daily dose (10 mg/kg qd, 130 mg/kg cumulative dose) of AZD5153.

Conclusions.

Here, we introduce a versatile and modular prodrug platform widely applicable to structurally diverse APIs as demonstrated in the context of two different BETis and 10 different linkers. One of these BETis, OTX-015, is a clinical compound; the other, T-API, is not suitable for translation due to poor drug-like properties. Thus, our platform can accelerate the development of both classes of compounds, which could have significant translational ramifications. Notably, despite extensive interest, no BET inhibitor has advanced to late-stage trials due to reported high-grade side effects[7] with the exception of CPI-0610, which is being investigated in the clinic for myelofibrosis, wherein its otherwise non-desirable activity in the bone marrow is being exploited. Similarly, many other promising drug candidates are often hindered from entering clinical practice by undesired toxicity to healthy cells, with 24% of drugs failing in clinical trials due to an inadequate clinical safety.[44] Furthermore, we demonstrate that by molecular tuning of linkers it is possible to achieve predictive correlation of *in vitro* release with *in vivo* performance, including sustained release of APIs at efficacious concentrations in tumor tissues while avoiding systemic exposure. Thus, by leverage the predictable BD and PK properties of the unique BPD scaffold, improved TIs can be readily achieved through passive targeting and linker design.

Finally, this work establishes the practicality of decoupling of physicochemical properties of an API from its biological activity. For example, we demonstrate how inherent poor physicochemical properties and rapid clearance of T-API can be turned into an advantage, potentially minimizing the toxicity of the drug molecules escaping into systemic circulation. A related strategy for managing cytopenia was evaluated using INCB054329,[46] a small molecule BET inhibitor reported to have a short half-life, but without a means to selectively target the drug to tumors, interpatient variability prevented identification of an effective dosing regimen and the trial was terminated. Collectively, our data suggest that the properties of BETi-BPDs warrant further investigation to enable potential clinical translation and that our BPD platform may be widely applicable across APIs to generate prodrugs with significantly improved TIs.

Supplementary Material

Refer to Web version on PubMed Central for supplementary material.

Author Manuscript Author Manuscript Author Manuscript Author Manuscript

Acknowledgements:

We thank Dr. Bruce Adams for assistance with NMR analysis, and Drs. Robert Langer, Rakesh Jain, and Ronald Evans for critical review and support of this work.

Funding: We thank XTuit Pharmaceuticals for support of this work. J.A.J. thanks the National Institutes of Health (1R01CA220468-01) for support.

References.

1. Lipinski CA; Lombardo F; Dominy BW; Feeney PJ, Experimental and computational approaches to estimate solubility and permeability in drug discovery and development settings. Adv. Drug Delivery Rev. 1997, 23 (1), 3–25.
2. Walters WP, Going further than Lipinski's rule in drug design. Expert Opinion on Drug Discovery 2012, 7 (2), 99–107. [PubMed: 22468912]
3. Hodgson J, ADMET—turning chemicals into drugs. Nat. Biotechnol. 2001, 19 (8), 722–726. [PubMed: 11479558]
4. Hann MM; Keserü GM, Finding the sweet spot: the role of nature and nurture in medicinal chemistry. Nat. Rev. Drug Discovery 2012, 11 (5), 355–365. [PubMed: 22543468]
5. Pritchard JF; Jurima-Romet M; Reimer MLJ; Mortimer E; Rolfe B; Cayen MN, Making Better Drugs: Decision Gates in Non-Clinical Drug Development. Nat. Rev. Drug Discovery 2003, 2 (7), 542–553. [PubMed: 12815380]
6. Alqahtani A; Choucair K; Ashraf M; Hammouda DM; Alloghbi A; Khan T; Senzer N; Nemunaitis J, Bromodomain and extra-terminal motif inhibitors: a review of preclinical and clinical advances in cancer therapy. Future Sci. OA 2019, 5 (3), FSO372. [PubMed: 30906568]
7. Mita MM; Mita AC, Bromodomain inhibitors a decade later: a promise unfulfilled? Br. J. Cancer 2020, 123 (12), 1713–1714. [PubMed: 32989227]
8. Cochran AG; Conery AR; Sims RJ, Bromodomains: a new target class for drug development. Nat. Rev. Drug Discovery 2019, 18 (8), 609–628. [PubMed: 31273347]
9. Kleppe M; Koche R; Zou L; van Galen P; Hill CE; Dong L; De Groote S; Papalexi E; Hanasoge Somasundara AV; Cordner K; Keller M; Farnoud N; Medina J; McGovern E; Reyes J; Roberts J; Witkin M; Rapaport F; Teruya-Feldstein J; Qi J; Rampal R; Bernstein BE; Bradner JE; Levine RL, Dual Targeting of Oncogenic Activation and Inflammatory Signaling Increases Therapeutic Efficacy in Myeloproliferative Neoplasms. Cancer Cell 2018, 33 (1), 29–43.e7. [PubMed: 29249691]
10. Delmore Jake E.; Issa Ghayas C.; Lemieux Madeleine E.; Rahl Peter B.; Shi J; Jacobs Hannah M.; Kastritis E; Gilpatrick T; Paranal Ronald M.; Qi J; Chesi M; Schinzel Anna C.; McKeown Michael R.; Heffernan Timothy P.; Vakoc Christopher R.; Bergsagel PL; Ghobrial Irene M.; Richardson Paul G.; Young Richard A.; Hahn William C.; Anderson Kenneth C.; Kung Andrew L.; Bradner James E.; Mitsiades Constantine S., BET Bromodomain Inhibition as a Therapeutic Strategy to Target c-Myc. Cell 2011, 146 (6), 904–917. [PubMed: 21889194]
11. Filippakopoulos P; Qi J; Picaud S; Shen Y; Smith WB; Fedorov O; Morse EM; Keates T; Hickman TT; Felletar I; Philpott M; Munro S; McKeown MR; Wang Y; Christie AL; West N; Cameron MJ; Schwartz B; Heightman TD; La Thangue N; French CA; Wiest O; Kung AL; Knapp S; Bradner JE, Selective inhibition of BET bromodomains. Nature 2010, 468 (7327), 1067–1073. [PubMed: 20871596]
12. Stathis A; Bertoni F, BET Proteins as Targets for Anticancer Treatment. Cancer Discov. 2018, 8 (1), 24–36. [PubMed: 29263030]
13. Fiskus W; Sharma S; Qi J; Shah B; Devaraj SGT; Leveque C; Portier BP; Iyer S; Bradner JE; Bhalla KN, BET Protein Antagonist JQ1 Is Synergistically Lethal with FLT3 Tyrosine Kinase Inhibitor (TKI) and Overcomes Resistance to FLT3-TKI in AML Cells Expressing FLT-ITD. Mol. Cancer Ther. 2014, 13 (10), 2315–2327. [PubMed: 25053825]
14. Kato F; Paolo Fiorentino F; Alibés A; Perucho M; Sánchez-Céspedes M; Kohno T; Yokota J, MYCL is a target of a BET bromodomain inhibitor, JQ1, on growth suppression efficacy in small cell lung cancer cells. Oncotarget 2016, 7 (47), 77378–77388. [PubMed: 27764802]

Author Manuscript Author Manuscript Author Manuscript Author Manuscript

15. Noel JK; Iwata K; Ooike S; Sugahara K; Nakamura H; Daibata M, Abstract C244: Development of the BET bromodomain inhibitor OTX015. Mol. Cancer Ther. 2013, 12 (11 Supplement), C244–C244.

16. Berthon C; Raffoux E; Thomas X; Vey N; Gomez-Roca C; Yee K; Taussig DC; Rezai K; Roumier C; Herait P; Kahatt C; Quesnel B; Michallet M; Recher C; Lokiec F; Preudhomme C; Dombret H, Bromodomain inhibitor OTX015 in patients with acute leukaemia: a dose-escalation, phase 1 study. Lancet Haematol. 2016, 3 (4), e186–e195. [PubMed: 27063977]

17. Lewin J; Soria J-C; Stathis A; Delord J-P; Peters S; Awada A; Aftimos PG; Bekradda M; Rezai K; Zeng Z; Hussain A; Perez S; Siu LL; Massard C, Phase Ib Trial With Birabresib, a Small-Molecule Inhibitor of Bromodomain and Extraterminal Proteins, in Patients With Selected Advanced Solid Tumors. J. Clin. Oncol. 2018, 36 (30), 3007–3014. [PubMed: 29733771]

18. Amorim S; Stathis A; Gleeson M; Iyengar S; Magarotto V; Leleu X; Morschhauser F; Karlin L; Broussais F; Rezai K; Herait P; Kahatt C; Lokiec F; Salles G; Facon T; Palumbo A; Cunningham D; Zucca E; Thieblemont C, Bromodomain inhibitor OTX015 in patients with lymphoma or multiple myeloma: a dose-escalation, open-label, pharmacokinetic, phase 1 study. Lancet Haematol. 2016, 3 (4), e196–e204. [PubMed: 27063978]

19. Wang JS-Z; Vita SD; Karlix JL; Cook C; Littlewood GM; Hattersley MM; Moorthy G; Edlund H; Fabbri G; Sachsenmeier KF; Davison C; Clark E; Moore KN; Bauer TM; Ulahannan SV; Patel MR; Hamilton EP, First-in-human study of AZD5153, a small molecule inhibitor of bromodomain protein 4 (BRD4), in patients (pts) with relapsed/refractory (RR) malignant solid tumor and lymphoma: Preliminary data. J. Clin. Oncol. 2019, 37 (15_suppl), 3085–3085.

20. Bradbury RH; Callis R; Carr GR; Chen H; Clark E; Feron L; Glossop S; Graham MA; Hattersley M; Jones C; Lamont SG; Ouvry G; Patel A; Patel J; Rabow AA; Roberts CA; Stokes S; Stratton N; Walker GE; Ward L; Whalley D; Whittaker D; Wrigley G; Waring MJ, Optimization of a Series of Bivalent Triazolopyridazine Based Bromodomain and Extraterminal Inhibitors: The Discovery of (3R)-4-[2-[4-[1-(3-Methoxy-[1,2,4]triazolo[4,3-b]pyridazin-6-yl)-4-piperidyl]phenoxy]ethyl]-1,3-dimethyl-piperazin-2-one (AZD5153). J. Med. Chem. 2016, 59 (17), 7801–7817. [PubMed: 27528113]

21. Shi J; Kantoff PW; Wooster R; Farokhzad OC, Cancer nanomedicine: progress, challenges and opportunities. Nat. Rev. Cancer 2016, 17, 20. [PubMed: 27834398]

22. Tran S; DeGiovanni P-J; Piel B; Rai P, Cancer nanomedicine: a review of recent success in drug delivery. Clin. Transl. Med. 2017, 6 (1), 44. [PubMed: 29230567]

23. Tyler DS; Vappiani J; Cañeque T; Lam EYN; Ward A; Gilan O; Chan Y-C; Hienzsch A; Rutkowska A; Werner T; Wagner AJ; Lugo D; Gregory R; Ramirez Molina C; Garton N; Wellaway CR; Jackson S; MacPherson L; Figueiredo M; Stolzenburg S; Bell CC; House C; Dawson S-J; Hawkins ED; Drewes G; Prinjha RK; Rodriguez R; Grandi P; Dawson MA, Click chemistry enables preclinical evaluation of targeted epigenetic therapies. Science 2017, 356 (6345), 1397–1401. [PubMed: 28619718]

24. Shi J; Vakoc Christopher R., The Mechanisms behind the Therapeutic Activity of BET Bromodomain Inhibition. Mol. Cell 2014, 54 (5), 728–736. [PubMed: 24905006]

25. Cochran AG; Conery AR; Sims RJ, Bromodomains: a new target class for drug development. Nat. Rev. Drug Discovery 2019, 18, 609–628. [PubMed: 31273347]

26. Xu Y; Vakoc CR, Targeting Cancer Cells with BET Bromodomain Inhibitors. Cold Spring Harb. Perspect. Med. 2017, 7, a026674. [PubMed: 28213432]

27. Love JA; Morgan JP; Trnka TM; Grubbs RH, A Practical and Highly Active Ruthenium-Based Catalyst that Effects the Cross Metathesis of Acrylonitrile. Angew. Chem. Int. Ed. 2002, 41 (21), 4035–4037.

28. Kawamoto K; Zhong M; Wang R; Olsen BD; Johnson JA, Loops versus Branch Functionality in Model Click Hydrogels. Macromolecules 2015, 48 (24), 8980–8988.

29. Johnson JA; Lu YY; Burts AO; Xia Y; Durrell AC; Tirrell DA; Grubbs RH, Drug-Loaded, Bivalent-Bottle-Brush Polymers by Graft-through ROMP. Macromolecules 2010, 43 (24), 10326–10335. [PubMed: 21532937]

30. Nguyen HVT; Gallagher NM; Vohidov F; Jiang Y; Kawamoto K; Zhang H; Park JV; Huang Z; Ottaviani MF; Rajca A; Johnson JA, Scalable Synthesis of Multivalent Macromonomers for ROMP. ACS Macro Lett. 2018, 7 (4), 472–476. [PubMed: 30271675]

Author Manuscript Author Manuscript Author Manuscript Author Manuscript

31. Vohidov F; Milling LE; Chen Q; Zhang W; Bhagchandani S; Nguyen, Hung VT; Irvine DJ; Johnson JA, ABC triblock bottlebrush copolymer-based injectable hydrogels: design, synthesis, and application to expanding the therapeutic index of cancer immunochemotherapy. Chem. Sci. 2020, 11 (23), 5974–5986. [PubMed: 34094088]
32. Golder MR; Liu J; Andersen JN; Shipitsin MV; Vohidov F; Nguyen HVT; Ehrlich DC; Huh SJ; Vangamudi B; Economides KD; Neenan AM; Ackley JC; Baddour J; Paramasivan S; Brady SW; Held EJ; Reiter LA; Saucier-Sawyer JK; Kopesky PW; Chickering DE; Blume-Jensen P; Johnson JA, Reduction of liver fibrosis by rationally designed macromolecular telmisartan prodrugs. Nat. Biomed. Eng. 2018, 2 (11), 822–830. [PubMed: 30918745]
33. Yeh TC; O'Connor G; Petteruti P; Dulak A; Hattersley M; Barrett JC; Chen H, Identification of CCR2 and CD180 as Robust Pharmacodynamic Tumor and Blood Biomarkers for Clinical Use with BRD4/BET Inhibitors. Clin. Cancer. Res. 2017, 23 (4), 1025–1035. [PubMed: 28073847]
34. Waring MJ; Chen H; Rabow AA; Walker G; Bobby R; Boiko S; Bradbury RH; Callis R; Clark E; Dale I; Daniels DL; Dulak A; Flavell L; Holdgate G; Jowitt TA; Kikhney A; McAlister M; Méndez J; Ogg D; Patel J; Petteruti P; Robb GR; Robers MB; Saif S; Stratton N; Svergun DI; Wang W; Whittaker D; Wilson DM; Yao Y, Potent and selective bivalent inhibitors of BET bromodomains. Nat. Chem. Biol. 2016, 12, 1097. [PubMed: 27775716]
35. Staben LR; Koenig SG; Lehar SM; Vandlen R; Zhang D; Chuh J; Yu S-F; Ng C; Guo J; Liu Y; Fourie-O'Donohue A; Go M; Linghu X; Segraves NL; Wang T; Chen J; Wei B; Phillips GDL; Xu K; Kozak KR; Mariathasan S; Flygare JA; Pillow TH, Targeted drug delivery through the traceless release of tertiary and heteroaryl amines from antibody–drug conjugates. Nat. Chem. 2016, 8, 1112. [PubMed: 27874860]
36. Burke PJ; Hamilton JZ; Pires TA; Setter JR; Hunter JH; Cochran JH; Waight AB; Gordon KA; Toki BE; Emmerton KK; Zeng W; Stone IJ; Senter PD; Lyon RP; Jeffrey SC, Development of Novel Quaternary Ammonium Linkers for Antibody–Drug Conjugates. Mol. Cancer Ther. 2016, 15 (5), 938–945. [PubMed: 26944920]
37. Greenwald RB; Pendri A; Conover CD; Zhao H; Choe YH; Martinez A; Shum K; Guan S, Drug Delivery Systems Employing 1,4- or 1,6-Elimination: Poly(ethylene glycol) Prodrugs of Amine-Containing Compounds. J. Med. Chem. 1999, 42 (18), 3657–3667. [PubMed: 10479297]
38. Conover CD; Zhao H; Longley CB; Shum KL; Greenwald RB, Utility of Poly(ethylene glycol) Conjugation To Create Prodrugs of Amphotericin B. Bioconj. Chem. 2003, 14 (3), 661–666.
39. Greenwald RB, PEG drugs: an overview. J. Controlled Release 2001, 74 (1), 159–171.
40. Greenwald RB; Choe YH; McGuire J; Conover CD, Effective drug delivery by PEGylated drug conjugates. Adv. Drug Delivery Rev. 2003, 55 (2), 217–250.
41. Ekladious I; Colson YL; Grinstaff MW, Polymer-drug conjugate therapeutics: advances, insights and prospects. Nat. Rev. Drug Discov. 2019, 18 (4), 273–294. [PubMed: 30542076]
42. Duncan R, Polymer conjugates as anticancer nanomedicines. Nat. Rev. Cancer 2006, 6 (9), 688–701. [PubMed: 16900224]
43. Rautio J; Meanwell NA; Di L; Hageman MJ, The expanding role of prodrugs in contemporary drug design and development. Nat. Rev. Drug Discov. 2018, 17 (8), 559–587. [PubMed: 29700501]
44. Harrison RK, Phase II and phase III failures: 2013–2015. Nat. Rev. Drug Discov. 2016, 15, 817. [PubMed: 27811931]
45. Wang D; Zou L; Jin Q; Hou J; Ge G; Yang L, Human carboxylesterases: a comprehensive review. Acta Pharmaceutica Sinica B 2018, 8 (5), 699–712. [PubMed: 30245959]
46. Liu PC; Liu XM; Stubbs MC; Maduskuie T; Sparks R; Zolotarjova N; Li J; Wen X; Favata M; Feldman P; Volgina A; DiMatteo D; Collins R; Falahatpisheh N; Polam P; Li Y; Covington M; Diamond-Fosbenner S; Wynn R; Burn T; Vaddi K; Yeleswaram S; Combs AP; Yao W; Huber R; Scherle P; Hollis G, Abstract 3523: Discovery of a novel BET inhibitor INCB054329. Cancer Res. 2015, 75 (15 Supplement), 3523–3523.

Author Manuscript Author Manuscript Author Manuscript Author Manuscript

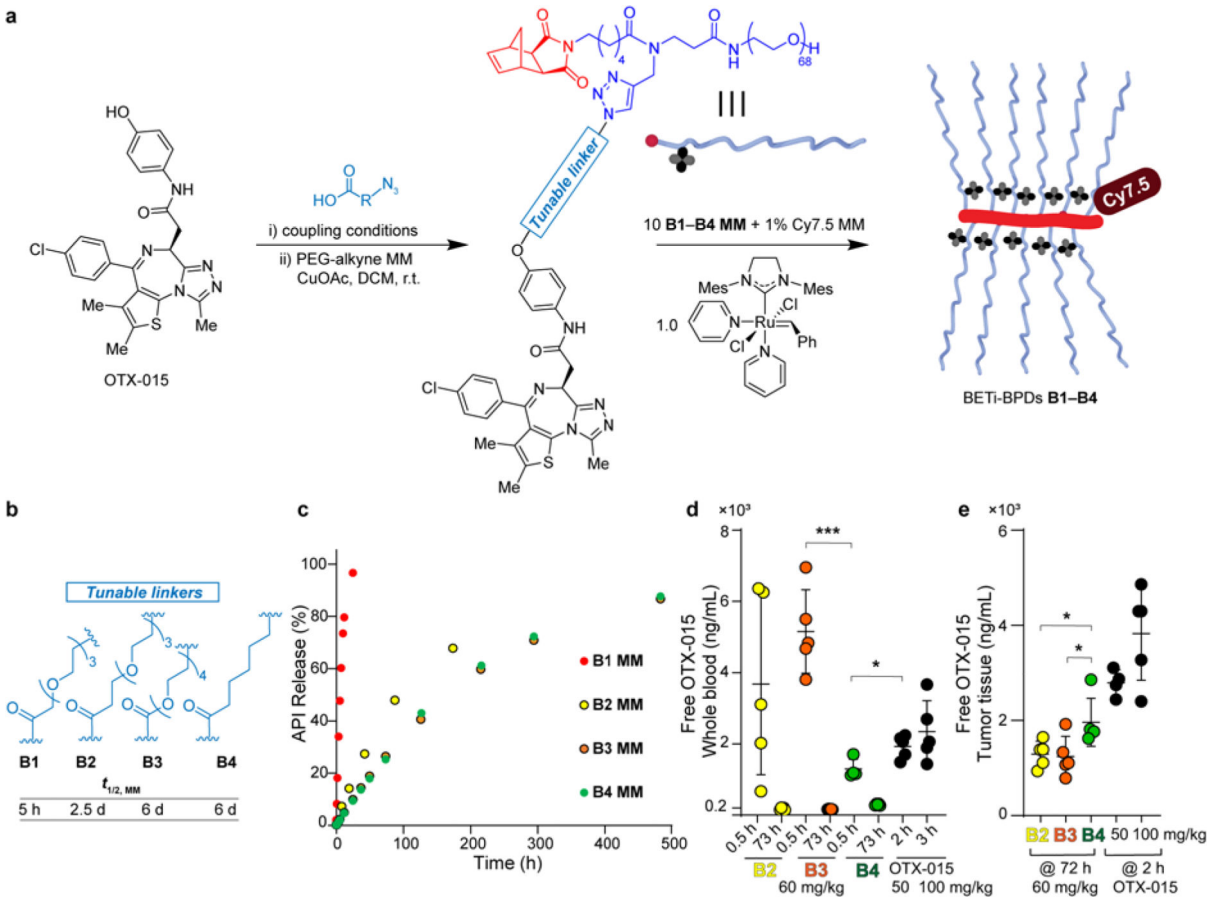

Figure 1. Design, synthesis, and OTX-015 release profiles for BETi-BPDs B1–B4.

(a) Design and synthesis of OTX-015-based brush prodrugs **B1–B4**. Azido-acids (shown in blue) are used to form ester or carbonate conjugates with OTX-015. Cu-catalyzed azide-alkyne cycloaddition to a PEG-alkyne macromonomer (MM) generates **B1–B4 MM**s. Ring-opening metathesis polymerization (ROMP) of each MM in the presence of a Cy7.5-labeled MM (1 mol %) generates BETi-BPDs **B1–B4**. **(b)** Careful linker design enables modulation of OTX-015 release half-lives. **(c)** Release of BET inhibitors *in vitro* (saline buffer, 37 °C). **(d)** Linker composition modulates serum stability. Blood levels of free OTX-015 drug released from **B4** at peak concentration (0.5 h post administration) is lower than the peak concentrations observed after equivalent doses of **B2**, **B3**, and lower compared to the maximum tolerated p.o. dose of OTX-015 at 2 or 3 h. **(e) B4** displays higher levels of released OTX-015 in tumor tissue compared to **B2** and **B3**, 72 hours after last dose of brush prodrugs. Statistical analysis performed using unpaired *t* test. Any p-values not shown are n.s.; * $p<0.05$, *** $p<0.001$; error bars represent SD.

Author Manuscript Author Manuscript Author Manuscript Author Manuscript

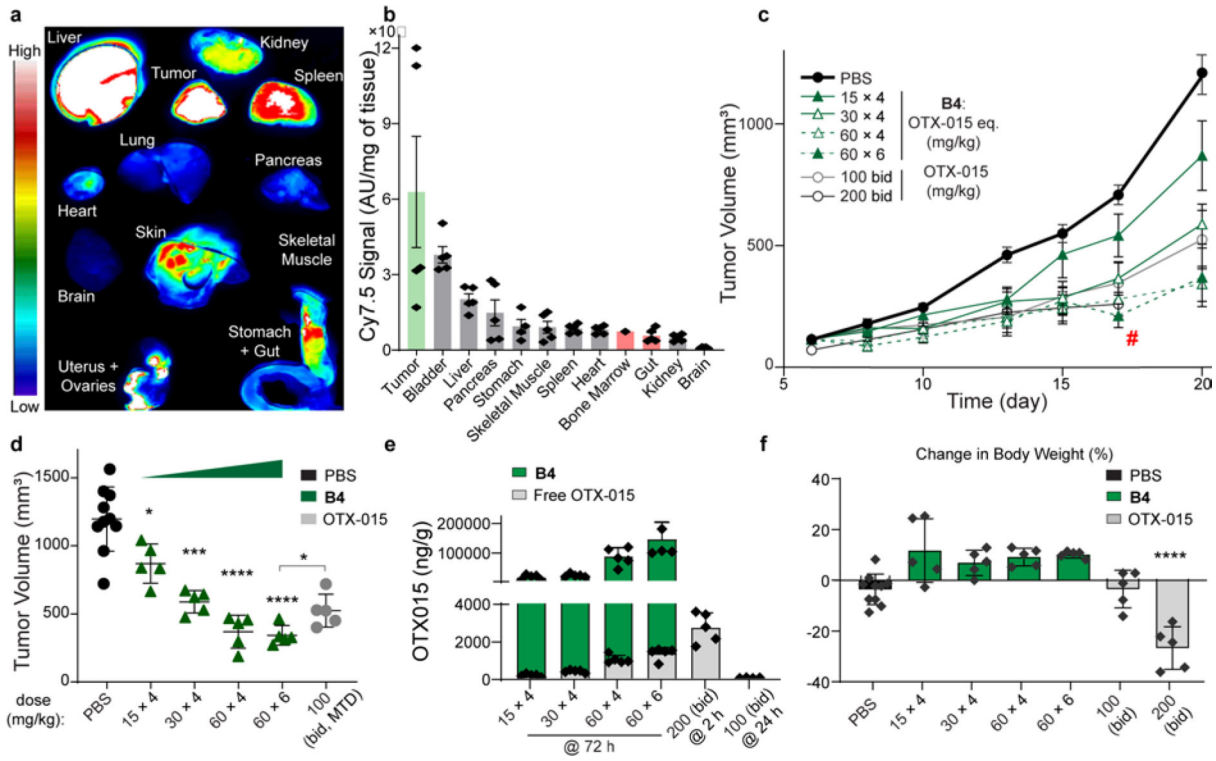

Figure 2. Tissue imaging and PK/PD/Efficacy studies of BETi-BPDs releasing OTX-015.

(a) Representative whole organ fluorescent imaging of Cy7.5-labled **B4** in tumor and indicated organs (Cy7.5 IVIS; $\lambda_{ex/em}$ = 745/800 nm). **(b)** Biodistribution of **B4** quantified using fluorescence signal (n=5) in homogenized tissue samples normalized by tissue weight; gut and bone marrow labeled in red font to highlight their low biodistribution; error bars represent SE. **(c)(d)** Anti-tumor efficacy in 4T1 orthotopic breast carcinoma model (Balb/C mice). **B4** was dosed i.v. with equivalents of OTX-015 at 15 mg/kg, 30 mg/kg, or 60 mg/kg, twice per week for two weeks for a total of 4 doses, or at 60 mg/kg every other day for two weeks for a total of 6 doses to mice (n=5 pr group) randomized with pre-treatment tumor sizes of 100 mm^3 (BPDs contain ~12% wt. of OTX-015; 500 mg/kg dose BPD is 60 mg/kg API equivalent). OTX-015 was dosed twice daily by oral gavage (bid; po). **(e)** Tumor PK of **B4** prodrug. BETi-BPD provides sustained release of API at the tumor site, and the levels of free OTX-015 at 72 h after injection are close to 50% of the peak concentration of the parent drug OTX-015 2 h are an oral dosage of 200 mg/kg bid. **(f)** No weight loss was observed in any of the **B4** regimens, while the maximum tolerated dose of API (100 mg/kg) caused diarrhea and some weight loss. #: The OTX-015 200-mg/kg bid cohort was taken down after eleven days due severe weight loss.

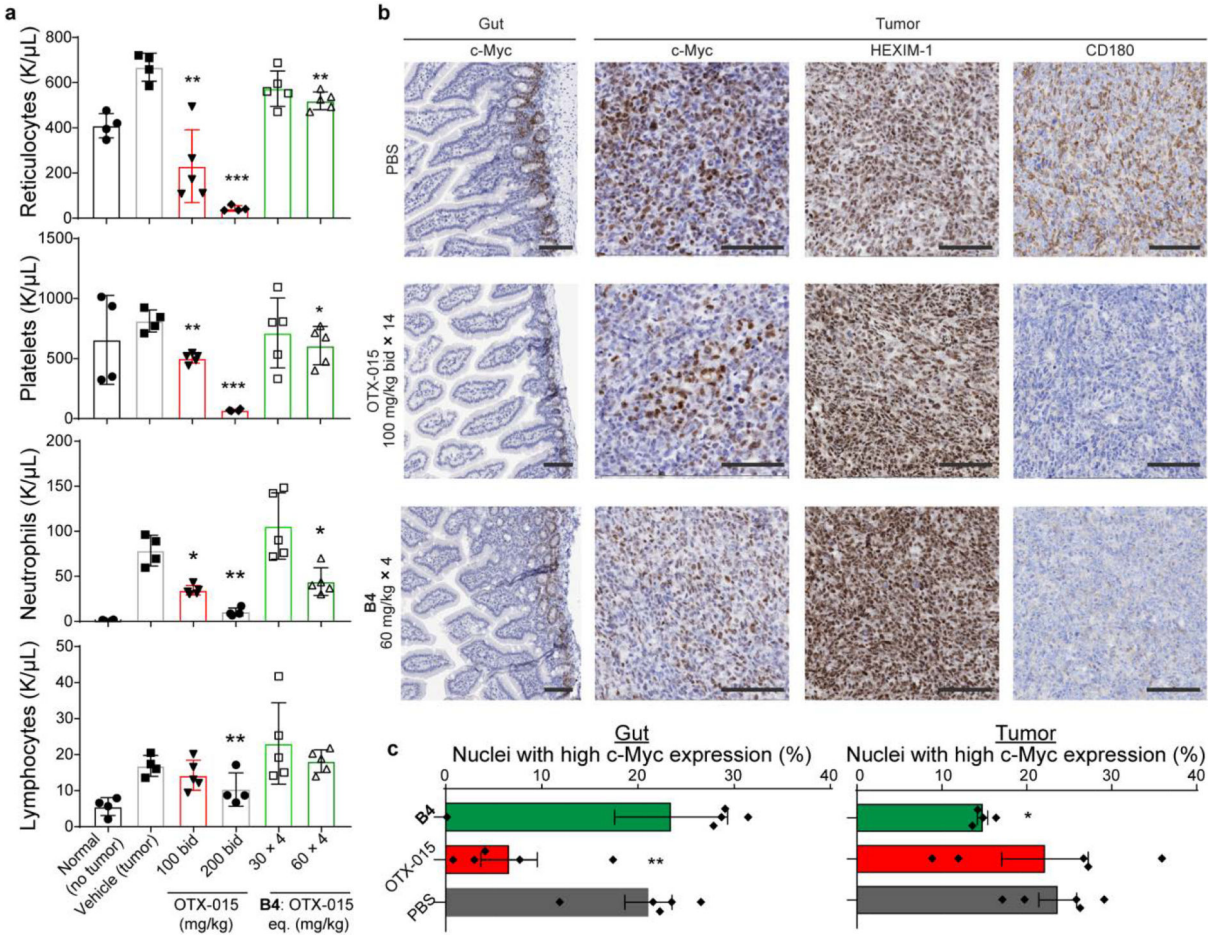

Figure 3. Blood cell populations and gut versus tumor biomarker assessments of B4 and OTX-015.

(a) Analysis of blood cell populations demonstrates that unlike the parent free OTX-015 drug, the **B4** prodrug does not cause the systemic toxicity associated with BET inhibition. No reduction in platelet, reticulocyte, neutrophil, and lymphocyte levels were detected (n=5) at doses resulting in superior anti-tumor efficacy of **B4** compared to free API; error bars represent SD. **(b)(c) B4** causes only minimal intestinal toxicity compared to OTX-015 as evidenced by in situ protein expression of c-Myc, a PD biomarker for BET inhibition, in the base of crypts and preserved colonic villus epithelial surface morphology. Anti-tumor efficacy of **B4** prodrug is comparable to free OTX-015 as shown by modulation of PD markers c-Myc, HEXIM1, and CD180 levels in extracted tumors. Statistical analysis performed using unpaired *t* test for tumor volumes and c-Myc expression and using Welch's *t* test for assessment of hematologic toxicity; all groups compared to the vehicle group except where indicated otherwise. Any p-values not shown are n.s.; * $p<0.05$, ** $p<0.01$, *** $p<0.001$, **** $p<0.001$. Scale bars: 100 μm.

Author Manuscript Author Manuscript Author Manuscript Author Manuscript

Author Manuscript Author Manuscript Author Manuscript Author Manuscript

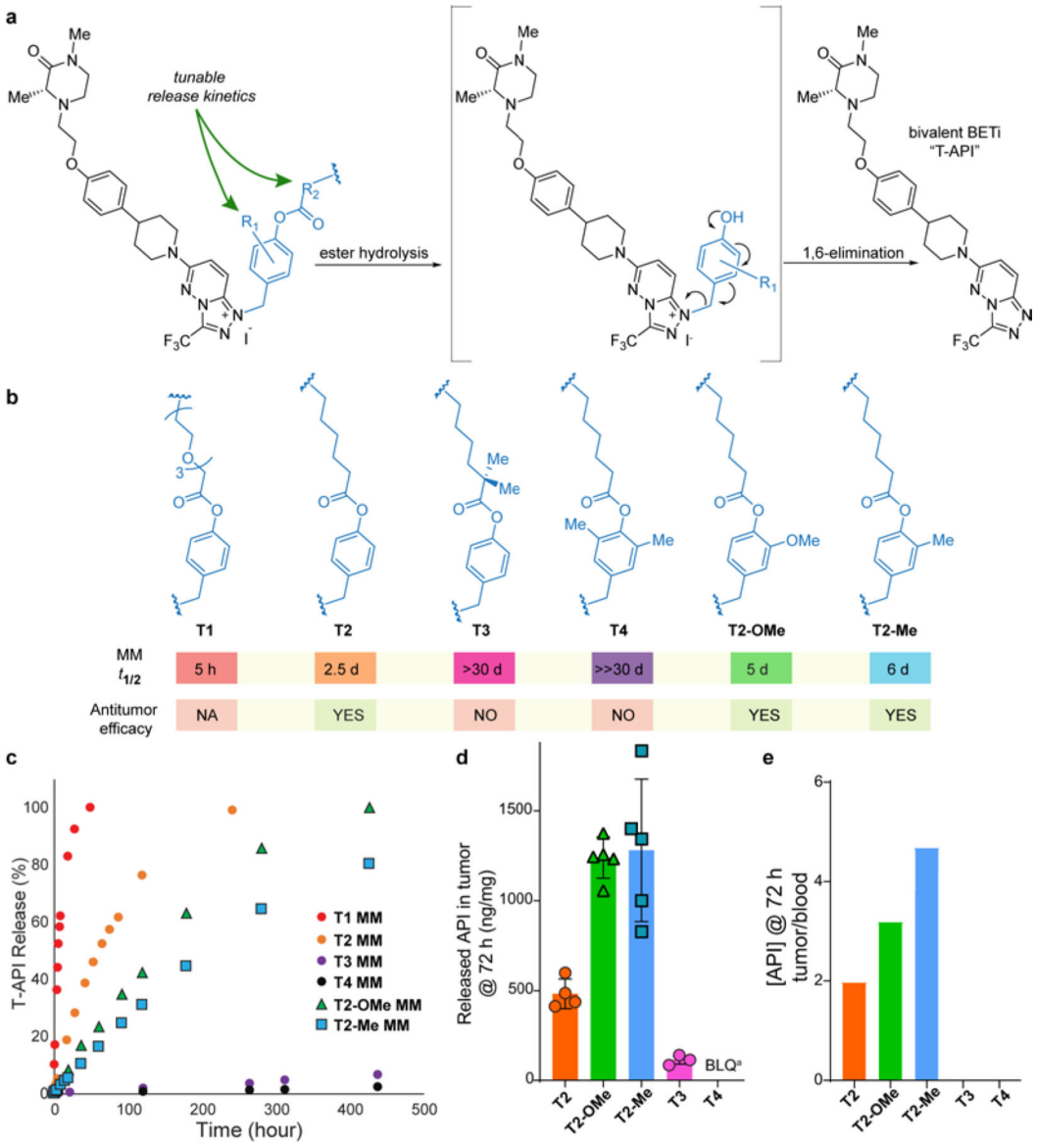

Figure 4. Phenyl ester traceless linker editing for optimized T-API release.

a, Drug release mechanism via 1,6-elimination from triazolopyridazinium salts conjugates in **T**-series brush prodrugs. **b,** Modulation of release kinetics of the T-API via linker chemistry. **c,** Release of T-API inhibitor *in vitro* (saline buffer, 37 °C). **d,** Released T-API in tumors 72 h after the last dose in 60 mg/kg × 4 treatment groups (n=5). Concentration of released T-API at the tumor site is finely tuned via linker chemistry; error bars represent SD. **e,** Ratios of released T-API in the tumor relative to whole blood. Brush prodrugs offer favorable accumulation and differential release in the tumor. [a]: below limit of quantification.

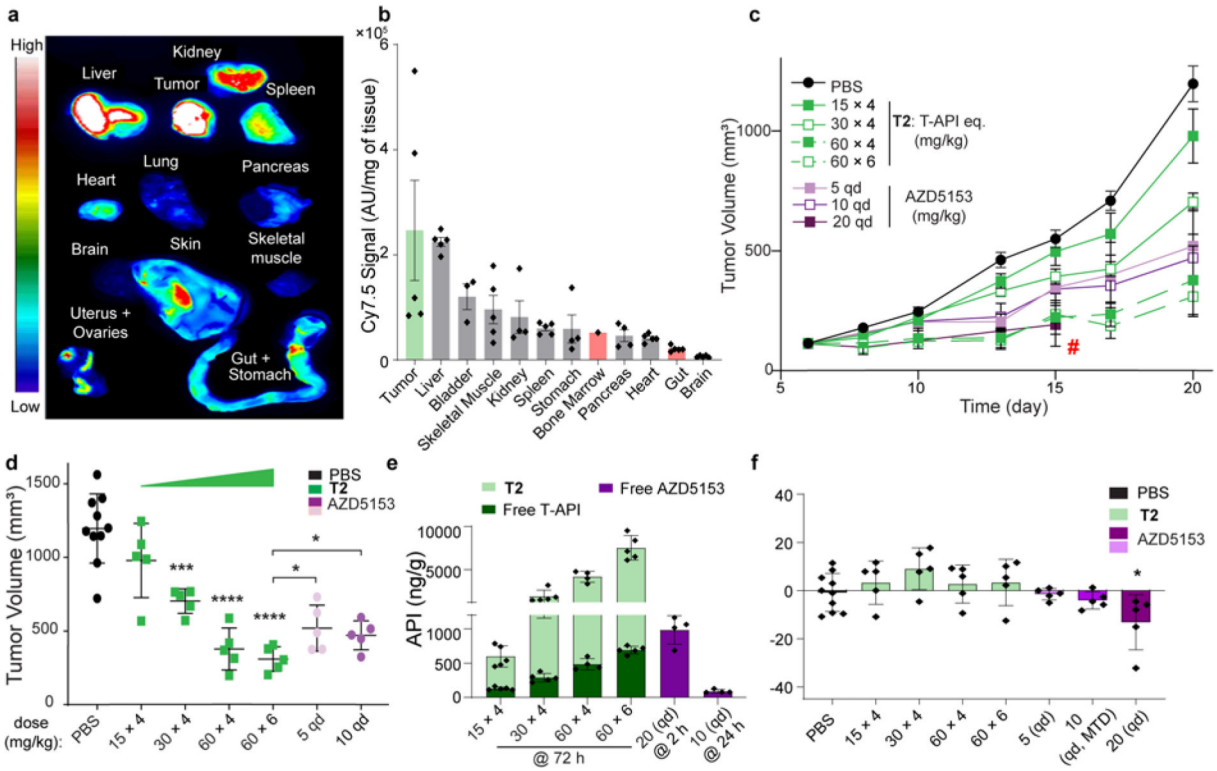

Figure 5. Tissue imaging and PK/PD/Efficacy studies of BETi-BPDs releasing the AZD5153-derivative T-API.

a, Representative whole organ Cy7.5 fluorescent imaging showing favorable accumulation of the **T2** prodrug in tumor. **b,** Biodistribution of the **T2** quantified using fluorescence signal (n=5) in homogenized tissue samples normalized by tissue weight; gut and bone marrow labeled in red font to highlight their low biodistribution; error bars represent SE. **c,d,** Efficacy in 4T1 orthotopic breast carcinoma model in Balb/C mice. **T2** was dosed with T-API equivalents at 15 mg/kg, 30 mg/kg, or 60 mg/kg, twice per week for two weeks for a total of 4 doses, or at 60 mg/kg every other day for two weeks for a total of 6 doses to mice randomized with tumor sizes of 100 mm^3 (BPDs contain ~12% wt. of T-API; 500 mg/kg dose BPD is 60 mg/kg API equivalent). AZD5153 was dosed qd as a PO bolus. **e,** Tumor pharmacokinetics of **T2** Brush prodrug. Brush provides sustained release of T-API at the tumor site, and the levels of free active drug at 72h after injection are comparable to the peak concentration of tumor AZD5153 (at 2 h post dosing) at the non-tolerated dosage of 20 mg/kg qd. **f,** No significant weight loss was observed in any of the **T2** regimens, while the highest tolerated dose of API at 10 mg/kg caused diarrhea and showed some weight loss. #: AZD5153 20-mg/kg cohort was taken down after ten days due severe weight loss.

Author Manuscript Author Manuscript Author Manuscript Author Manuscript

Author Manuscript Author Manuscript Author Manuscript Author Manuscript

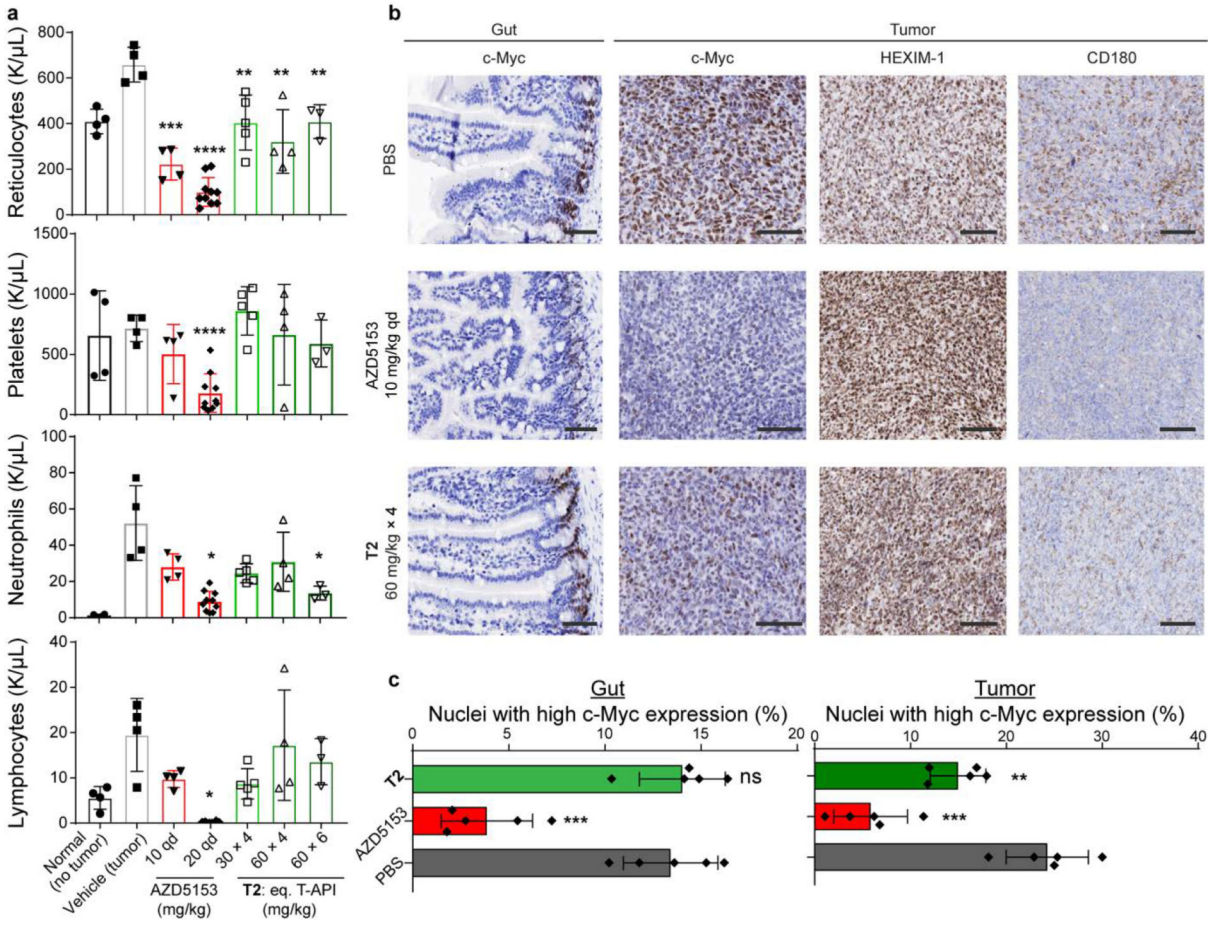

Figure 6. Blood cell counts and gut versus tumor biomarker assessments of T2 and AZD5153.

(a) Analysis of blood cell populations demonstrates that, unlike free AZD5153, **T2** Brush prodrug does not cause systemic toxicity normally associated with BET inhibition in bone marrow. No reduction in platelet, reticulocyte, neutrophil, and lymphocyte levels were detected (n=5) at doses resulting in superior anti-tumor efficacy of **T2** compared to free AZD5153; error bars represent SD. **h,i, T2** causes only minimal intestinal toxicity compared to OTX-015 as evidenced by *in situ* protein expression of c-Myc, biomarker for BET inhibition, in the base of crypts and preserved colonic villus epithelial surface morphology. Anti-tumor efficacy of **T2** prodrug is comparable to free AZD5153 as shown by modulation of PD markers c-Myc, HEXIM1, and CD180 levels in extracted tumors. Statistical analysis performed using unpaired *t* test for tumor volumes and c-Myc expression and using Welch's *t* test for assessment of hematologic toxicity; all groups compared to the vehicle group except where indicated otherwise. Any p-values not shown are n.s.; * $p<0.05$, ** $p<0.01$, *** $p<0.001$, **** $p<0.0001$. Scale bars: 100 μm.

Author Manuscript Author Manuscript Author Manuscript Author Manuscript

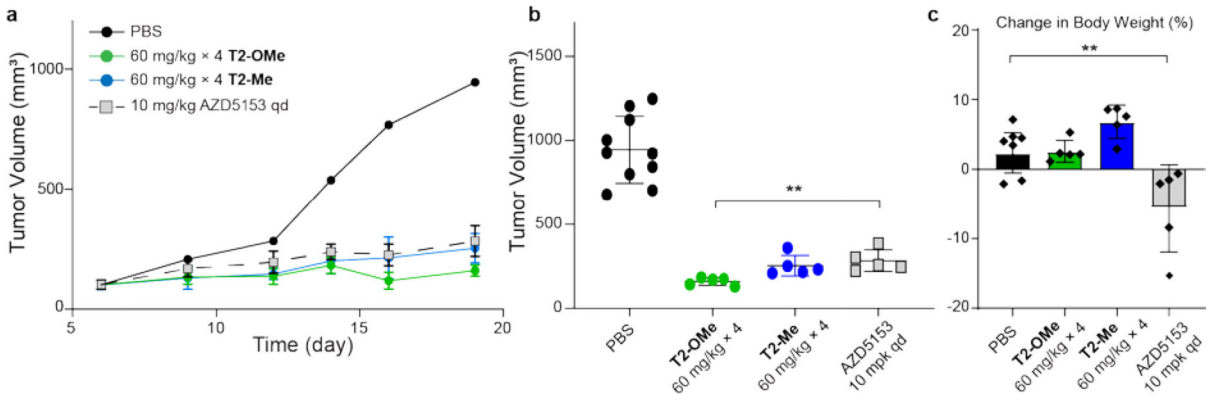

Figure 7.

a,b, Brush prodrugs **T2-OMe** and **T2-Me** display improved tumor growth inhibition after fewer doses compared to AZD5153. BPDs were dosed at 60 mg/kg equivalent of T-API twice per week for two weeks for a total of 4 doses to Balb/C mice bearing 4T1 orthotopic tumors; AZD5153 was dosed at 10 mg/kg qd as a PO bolus. **c,** No significant weight loss was observed in any of the **T2-Ome** and **T2-Me** regimens, while the highest tolerated dose of API at 10 mg/kg caused diarrhea and showed some weight loss. Error bars represent SD. Statistical analysis performed using unpaired *t* test; * $p<0.05$, ** $p<0.01$.